Synthesis and Characterization of Lithium-Ion Conductive Membranes with Low Water Permeation

David A. Stone, Daniel T. Welna, and Harry R. Allcock*

Department of Chemistry, The Pennsylvania State University, University Park, Pennsylvania 16802

Received October 23, 2006. Revised Manuscript Received February 19, 2007

Three polymer systems were investigated in an attempt to produce lithium-ion conductive polymers that resist the absorption of water. All were synthesized via ring-opening metathesis polymerization (ROMP) to give a polynorbornene backbone, with each repeat unit bearing a pendent cyclotriphosphazene ring. Each pendent inorganic ring carried hydrophilic, ion conductive 2-(2-methoxyethoxy)ethoxy, and/or hydrophobic 2,2,2-trifluoroethoxy side groups. The three systems were (a) composite blends of two polymers with all hydrophobic and all lithium ion conductive side groups, (b) homopolymers in which each polymer repeating unit bore both hydrophobic and ion conductive side groups, or (c) copolymers derived from two monomers, one of which bore only hydrophobic side groups and the other with all ion conductive groups. Room-temperature (25 °C) ionic conductivities were measured by incorporating 7 mol % $LiBF_4$ in each system. Hydrophobicity was estimated from water-contact angles of the polymeric materials with and without $LiBF_4$. One of the homopolymer systems with two methoxyethoxyethoxy and three trifluoroethoxy groups on every side group generated conductivities in the range of 1.2×10^{-5} S/cm at 25 °C in combination with a semihydrophobic surface with a water-contact angle of 77.7 °. The conductivity of this polymer was close to that of the highly hydrophilic, water-soluble poly[bis(2-(2-methoxyethoxy)ethoxy)phosphazene] (MEEP), which is one of the most conductive solid polymer electrolytes (2.7×10^{-5} S/cm at 25 °C).[5]

Introduction

Both primary and secondary lithium batteries are important components of mobile devices. Metallic lithium has a high energy density, low equivalent weight, and a large standard reduction potential (−3.04 V), which make it an ideal candidate for a battery anode material. Indeed, lithium batteries are considered to have the most promise for future battery technologies, and significant advantages are foreseen for batteries that are based on solid polymer or gel electrolyte systems.[1] Among the challenges that hinder future progress in this field is the need to prevent the ingress of water into lithium batteries, especially for devices that operate in humid and marine environments and where reduction of weight and compact design are crucial requirements.[2−8]

This challenge has been circumvented in some laboratories by the use of magnesium or aluminum anodes, which do not react violently with water and are capable of generating current in experimental batteries.[6,7,8] However, these metals lack the energy and power density of lithium and must be considered as compromise devices.

Thus, an extreme challenge is to design a polymer electrolyte for primary lithium batteries that are activated by immersion in seawater.[2−5] Such an electrolyte must conduct lithium ions but prevent water from penetrating through the polymer to react with the lithium metal anode. Unfortunately, those polymers that are good cation conductors are nearly always highly hydrophilic, whereas most hydrophobic polymers are poor ion conductors. Thus, the design of a suitable membrane electrolyte requires a balancing of two opposing characteristics. The work described here is an attempt to find that balance.

Earlier work in our program demonstrated the utility of linear phosphazene polymers that have oligoethyleneoxy side chains for lithium ion conduction in secondary lithium batteries.[9,10] Inoue and co-workers[11] developed a pendent phosphazene bearing ionic conductive groups with similar results. The etheric oxygen atoms in the side groups provide coordination sites that facilitate cation hopping and salt solvation. Although these polymers provide adequate solid-

* Corresponding author. E-mail: hra@chem.psu.edu.

(1) Brandt, K. *Solid State Ionics* **1994**, *69*, 173.
(2) Wu, Y. P.; Jiang, C.; Wan, C.; Holze, R. *Carbon* **2003**, *41*, 437.
(3) (a)Trommsdorff, E.; Köhle, H, Lagally, P. *Makromol. Chem.* **1947**, *1*, 169.; (b) Urquidi-Macdonald, M.; Castaneda, H.; Cannon, A. M. *Electrochim. Acta* **2002**, *47*, 2495.
(4) Zhang, Y.; Urquidi-Macdonald, M. *J. Power Sources* **2005**, *144*, 191.
(5) Zhang, Y.; Urquidi-Macdonald, M. *J. Power Sources* **2004**, *129*, 312.
(6) Wilcock, W. S. D.; Kauffman, P. C. *J. Power Sources* **1997**, *66*, 71.
(7) Medeiros, M. G. *J. Power Sources* **1999**, *80*, 78.
(8) Hasvold, Ø.; Henriksen, H.; Melvær, E.; Citi, G.; Johansen, B. Ø.; Kjonigsen, T.; Galetti, R. *J. Power Sources* **1997**, *65*, 253.
(9) Blonsky, P. M.; Shriver, D. F.; Austin, P. E.; Allcock, H. R. *J. Am. Chem. Soc.* **1984**, *106*, 6854.
(10) Allcock, H. R.; Austin, P. E.; Neenan, T. X.; Sisko, J. T.; Blonsky, P. M.; Shriver, D. F. *Macromolecules* **1986**, *19*, 1508. Blonsky, P. M.; Shriver, D. F.; Austin, P. E.; Allcock, H. R. *Polym. Mater. Sci. Eng.* **1985**, *53*, 118. Blonsky, P. M.; Shriver, D. F.; Austin, P. E.; Allcock, H. R. *Solid State Ionics* **1986**, *18*, 258. Nelson, C. J.; Coggio, W. D.; Allcock, H. R. *Chem. Mater.* **1991**, *3*, 786. Allcock, H. R.; O'Connor, S. J. M.; Olmeijer, D. L.; Napierala, M. E.; Cameron, C. G. *Macromolecules* **1996**, *29*, 7544. Allcock, H. R.; Napierala, M. E.; Cameron, C. G.; O'Connor, S. J. M. *Macromolecules* **1996**, *29*, 1951.
(11) Inoue, K.; Nishikawa, Y.; Tanigaki, T. *Macromolecules* **1991**, *24*, 3464; Inoue, K.; Kinoshita, K.; Nakahara, H.; Tanigaki, T. *Macromolecules* **1990**, *23*, 1227.

10.1021/cm062528u CCC: $37.00
Published on Web 04/19/2007

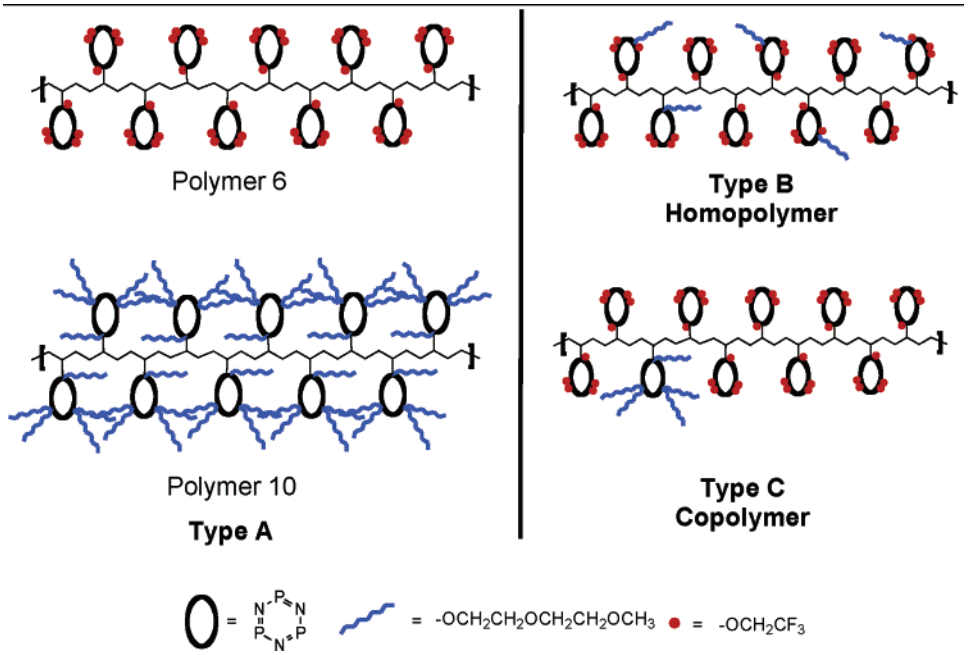

Figure 1. Illustration of polymer architectures.

state conductivity and excellent gel conductivity, they are hydrophilic or even soluble in water.

In other work, we have demonstrated the extreme hydrophobicity of fluorinated alkoxy groups linked to a polyphosphazene chain, and these polymers provide a significant barrier to water permeation.[12]

Our goal in this work was to combine the effects of these two side groups in a different type of polymer architecture based specifically on comb-type macromolecules with a hydrophobic polynorbornene backbone and cyclophosphazene rings linked to that backbone. Each phosphazene ring is a platform for some combination of methoxyethoxyethoxy and trifluoroethoxy groups. The use of pendent phosphazene rings as a platform for the active side groups allows a much higher concentration of active groups (five per repeating unit) compared to two per repeating unit in classical linear phosphazene polymers and most other macromolecules.

Three comb-type-polymer systems were targeted. They are described here as Type A (composite blends of two macromolecules, each with all oligoethyleneoxy or all trifluoroethoxy side units); Type B (homopolymers derived from monomers that bear both oligoethyleneoxy and trifluoroethoxy side groups); and Type C (copolymers derived from two monomers, one of which bears oligoethyleneoxy and the other trifluoroethoxy side chains). The hydrophobicity of the polymers was controlled by changing the ratio of hydrophobic to hydrophilic units. Figure 1 illustrates the differences between these systems.

In the Type A systems, the objective was to attempt to balance the two contradictory properties through either compatible blends or incompatible domain formation. Different ratios of the two homopolymers provided an opportunity to examine compatibility/incompatibility issues as well as hydrophobicity and ionic conductivity.

The Type B systems (mixed-substituent homopolymers), with both types of side group on every repeating unit, ensure compatibility of the two types of side groups at the molecular level. It also promised a homogeneous distribution of the two side groups throughout the polymer matrix, and ensured a uniform proximity of the ion conductive groups to each other.

Type C systems (copolymers), with different ratios of the two different single-substituent monomers, allowed comparisons to be made with the other two systems, with the added option to examine the effect of changes in the average proximity of ion conductive and hydrophobic units. In principle, Type C polymers are easier to synthesize because only two individual monomers are required to make a copolymer, regardless of the ratio. However, different polymerization reactivities for the two monomers can complicate polymer synthesis.

Results and Discussion

Synthesis of the Polymers. Synthesis of the polymers was accomplished through a four-step process. First, a norbornyl unit was linked to a short spacer group that was terminated by an alcohol moiety to give 5-norbornene-2-methanol (Figure 2). The potassium salt of this species was then employed to replace one of the chlorine atoms in hexachlorocyclotriphosphazene (**1**). Disubstitution of hexachlorocyclotriphosphazene at this stage was prevented by using less than one equivalent (0.7 eq) of the 5-norbornene-2-methanol and a low reaction temperature of −78 °C. Disubstitution would lead to polymer crosslinking. Subsequent removal by sublimation of unsubstituted hexachlorocyclotriphosphazene yielded pure mono-(5-norbornene-2-methoxy) pentachlorocyclotriphosphazene (**2**). The remaining five chlorine atoms on the phosphazene ring were subsequently replaced by the

(12) Allcock, H. R.; Kugel, R. L. *J. Am. Chem. Soc.* **1965**, *87*, 4216. Allcock, H. R.; Kugel, R. L.; Valan, K. J. *Inorg. Chem.* **1966**, *5*, 1709. Singh, A.; Steely, L.; Allcock, H. R. *Langmuir* **2005**, *21*, 11504. Allcock, H. R.; Steely, L. B.; Singh, A. *Polym. Int.* **2006**, *55*, 621.

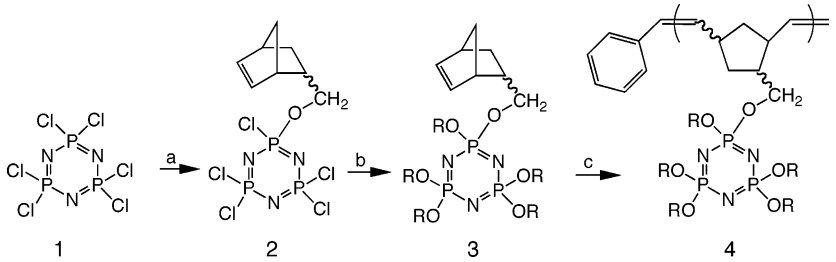

Figure 2. General route to mononorbornene pentasubstituted cyclotriphosphazene monomers.

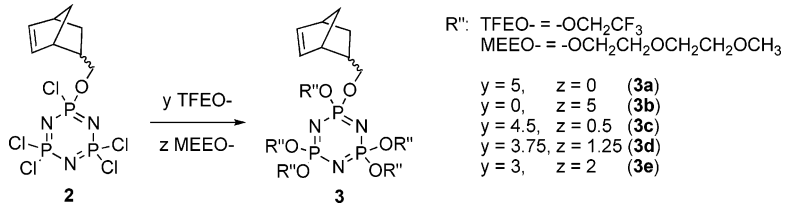

Figure 3. Type A and B monomer synthesis variations.

oligoethyleneoxy or trifluoroethoxy groups to give **3**. Finally, the norbornenyl units were polymerized with the use of a Grubbs ring-opening metathesis (ROMP) initiator, $[Cl_2Ru(PCy_3)_2(CH{=}CHPh)]$ to give **4**.[13,14]

Type A systems were derived by blending two homopolymers, themselves produced separately from two different monomers. In the first monomer, the five remaining chlorine atoms on the cyclophosphazene intermediate (**2**) were replaced by treatment with the sodium salt of 2,2,2-trifluoroethanol to produce monomer **3a**. The second monomer was synthesized via the corresponding reaction with the sodium salt of 2-(2-methoxyethoxy)ethanol to yield **3b**. Polymerization of the monomers was accomplished through the rapid addition of a solution of the initiator in methylene chloride to the monomer dissolved in THF. A monomer to initiator ratio of 250:1 was used for all polymerizations. The polymerization was allowed to proceed until a change in viscosity was detected. The polymerization time varied from monomer to monomer and ranged from several seconds to several minutes. Polymerizations that continued beyond this point yielded polymers that were difficult to redissolve after the initial solvent removal. This could be a consequence of chain entanglements and knots caused by the complex pendent groups. Each polymerization was terminated with ethyl vinyl ether. The polymer solutions were transferred to dialysis tubing (molecular weight cutoff 12 000−14 000) and dialyzed versus THF for 48 h, with the THF changed every 12 h. The polymer was then precipitated from solution into a nonsolvent such as hexanes, collected, and dried under vacuum at 60 °C for 24 h. These two single-substituent polymers are identified as **6** (100% trifluoroethoxy) and **10** (100% methoxyethoxyethoxy). Polymers **6** and **10** were subsequently mixed in the desired ratios to form polymers **14**−**16**.

Synthesis of the Type B homopolymers (Figure 3) began as before with the pentachlorophosphazene functional intermediate (**2**). Sodium salts of 2,2,2-trifluoroethanol and 2-(2-methoxyethoxy)ethanol were added together in the appropriate ratio to monomer intermediate (**2**) to yield disubstituted monomers **3c**, **3d**, and **3e**. The side group ratios were monitored by integration of the proton NMR signals. These monomers were clear, light brown liquids obtained in yields higher than 90% and in most cases as high as 98%. Polymerization conditions to give polymers **11**−**13** were the same as those described above.

Type C monomers were the same as those used for the Type A polymers (**6** and **10**), but were used to produce copolymers rather than separate homopolymers. Ring-opening metathesis of precise mixture of monomers **3a** and **3b** produced polymers **7**−**9** (Figure 4).

Polymer Properties. The mechanical properties of these comb-type polymers are influenced by the backbone length and the composition of the side groups.[3] Specific ratios of side groups were targeted in an attempt to maximize water impermeability and ionic conduction. All the polymers were immobile amorphous gums. Polymer **10** (with methoxyethoxyethoxy groups only) was the least dimensionally stable because of its low molecular weight. However, it did not undergo flow under the influence of gravity. Type B polymers were found to be more dimensionally stable than the Type C polymers.

NMR Characterization. Monomers **3a**−**3e** and salt-free polymers **6**−**13** were analyzed by ^1H and ^{31}P NMR spectroscopy. All the monomers consisted of a mixture of endo and exo isomers, which were distinguishable by $^1H-^{13}C$ HMQC NMR methods.

For the purpose of this work, all the macromolecules are assumed to possess a random statistical distribution of the different isomers. The final halogen-free polymers were also asymmetric and contain regioisomers from one repeat unit to another.[15] ^1H NMR spectra of the salt-free polymers showed broad resonances at ~5.0 ppm from vinyl protons. Significant peaks were also located between 1.2 and 3.0 ppm for non-olefinic protons. Additional peaks were detected at 4.26 ppm for both monomers and polymers that contained

(13) Allcock, H. R.; Laredo, W. R.; deDenus, C. R.; Taylor, J. P. *Macromolecules* **1999**, *32*, 7719.
(14) Allcock, H. R.; Laredo, W. R.; Kellam, E. C.; Morford, R. V. *Macromolecules* **2001**, *34*, 787.
(15) Ivin, K. J. *Olefin Metathesis and Polymerization Catalysts*; Kluwer Academic Publishers: Dordrecht, The Netherlands, 1990.

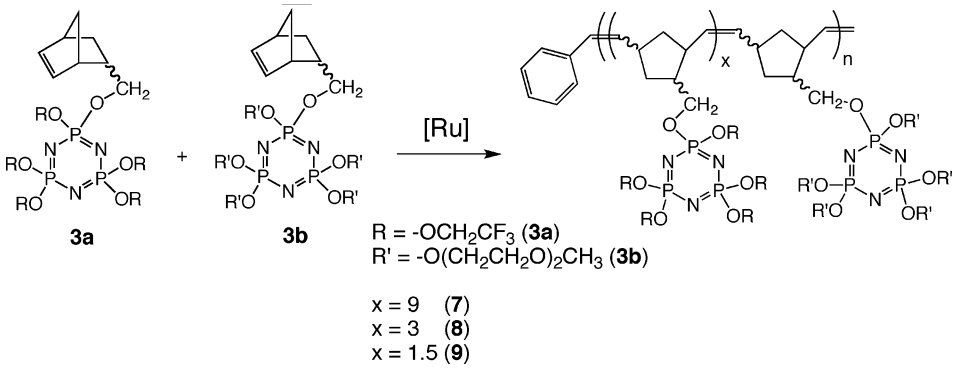

Figure 4. Type C polymerization.

Table 1. Characterization Data for Polymers 6−16[a]

polymer	MEEO %	TFEO %	$1 \times 10^{-3}\ M_w$[b]	$1 \times 10^{-3}\ M_n$[b]	PDI[b]
6	0	100	666	256	2.6
7	10	90	312	191	1.6
8	25	75	78.5	44	1.8
9	40	60	62.1	28	2.2
10	100	0	45.3	21	2.2
11	10	90	943	371	2.5
12	25	75	754	265	2.9
13	40	60	687	219	3.1
14	10	90	[c]	[c]	[c]
15	25	75	[c]	[c]	[c]
16	40	60	[c]	[c]	[c]

[a] Polymers were salt-free. [b] Determined by GPC using polystyrene standards. [c] Mixture of polymers **6** and **10**. MEEO = methoxyethoxyethoxy; TFEO = trifluoroethoxy.

trofluoroethoxy side groups. Peaks were also present between 4.0 and 3.3 ppm for the methoxyethoxyethoxy side groups located on the phosphazene rings in both monomers and polymers.

The electronic environment of the different side groups had a minimal effect on the ^{31}P NMR spectrum of the phosphazene rings in each monomer. All ^{31}P NMR shifts were centered at 17.5−18.0 ppm. The polymer structure gave significantly less splitting than the monomers. The splitting in the ^{31}P NMR spectra is a result of the different environments caused by the asymmetric substitution and the exo and endo isomers of the norbornene unit.

The ^{13}C NMR spectra of monomers **3a**−**3e** indicated the presence of vinyl protons between 138 and 132 ppm. Once polymerized, and the ring strain relieved, the peaks shifted to slightly lower values at 136−130 ppm. Significant spin−spin coupling in the ^{13}C NMR spectra was observed for $-CH_2CF_3$ and $-CH_2CF_3$ groups, with values of 39.6 and 278 Hz, respectively. The alkyl ether side groups gave singlet peaks located between 71.5 and 58.6 ppm (assignments given in the Experimental Section).

Molecular Weights. Average molecular weights of the salt-free polymers, determined by gel permeation chromatography, were between 4.5×10^5 and 67×10^5 g/mol. This corresponds to approximately 75−800 repeat units for different polymers. The polydispersity indices (PDIs) for the polymers ranged from 1.6 to 3.1 (Table 1), which is typical of ROMP type polymerizations. The monomer-to-initiator ratios and reaction times were used to control the molecular weights of the final polymers. However, attempts to maximize the molecular weights resulted in insoluble polymers. Long reaction times often lead to higher molecular weights, a result that can be explained by a pseudo-Trommsdorff effect.[3a] This phenomenon is also found in other norbornene-based ROMP polymers.[3b] Thus, to avoid this problem of high PDIs and poor solubility, most reaction times were kept well below 30 min. Each polymerization was terminated at a point based on the viscosity of the solution as described above.

Each polymer architecture, Type A, B, or C, was associated with significantly different molecular weights because of the different side group environments. The changes in hydrophilicity and hydrophobicity in the vicinity of the catalyst site undoubtedly affects the propagation and termination processes. Moreover, the length of the methoxyethoxyethoxy groups and their capacity to coordinate to electrophilic centers may also play a role in reducing the catalyst activity. Polymers **7** through **9** (Type C) show a significant decrease in molecular weight as the alkyl ether loading of the polymers increased. Moreover, polymers derived from monomer **3a** had higher molecular weights than those from **3b**, which indicates that the alkyl ether groups interfere with the polymerization process through steric or coordinative forces. Type B polymers had much higher molecular weights than polymers of Type C, probably a result of the more uniform chemical composition of the monomers.

Glass-Transition Temperatures. Differential scanning calorimetry was used to study both the salt-free and the salt-containing polymers. The salt-free **6**−**16** polymers had T_g values that ranged from 0.9 to −58.6 °C, and these reflected the transition-lowering characteristic of the alkyl ether groups. Specific values are shown in Table 2. In general, an increase in methoxyethoxyethoxy incorporation reduced the T_g. This is probably due to free volume effects caused by the presence of the longer, more flexible side groups.

The glass transitions of salt-containing polymers **6**−**16** containing 7 mol % $LiBF_4$ are reported in Table 2. The values are well below room temperature, with polymer **6** having the highest transition at −14.9 °C. All these polymers underwent a decrease in T_g with increasing alkyl ether incorporation. The addition of salt to the polymer system in general reduced the T_g of the polymers.

The salt-containing polymer blends of the two single-substituent polymers (Type A, **14**−**16**) showed multiple DSC transitions, which indicated significant phase separation. This behavior is attributed to the incompatibility of the side groups on the two polymers. Moreover, the glass-transition temperature of each homopolymer was below room temperature, which would aid in phase separation. The salt-free polymers

Table 2. Characterization Data for Polymers 6−16

	with $LiBF_4$			without $LiBF_4$	
polymer	T_g (°C)[a]	σ @ 25 °C (nS/cm)	WCA (deg)[b]	T_g (°C)[a]	WCA (deg)[b]
6	−14.9	1461	98.3	−13.6	111.5
7	−27.9	2106	91.3	−14.8	95.6
8	−28.5	3569	48.8	−18.5	60.5
9	−32.5	6973	36.2	−25.9	50.9
10	−50.9	13900	0[c]	−58.6	0[c]
11	−22.8	610	85.5	0.9	86.0
12	−31.9	2557	83.0	−23.7	83.0
13	−40.7	11776	77.7	−33.2	82.1
14	−59.8, −15.7	83	79 → 41[d]	−49.0	110 → 28.5[d]
15	−45.6, −7.1	302	72 → 40[d]	−29.0	94 → 65.0[d]
16	−50.0, −10.4	1961	68 → 38[d]	−37.7	75 → 29.0[d]

[a] Analysis by DSC with a scan rate of 10 °C/min. [b] Water contact angle determined through water-drop method. [c] Polymer **10** was soluble in water. [d] Water contact angles of polymers **14**−**16** decreased over the course of several minutes; initial and final values are reported.

showed a single glass transition. The T_g values ranged from −29.0 to −49.0 °C. The increase in the T_g of polymer **15** does not fit the general decreasing T_g trend.

The type B polymers with salt (**11**−**13**) show a distinct change in T_g with an increase in the methoxyethoxyethoxy incorporation. The T_g values ranged from −22.8 to −40.7 °C for polymers **7**−**9**. Type B architectures have the methoxyethoxyethoxy units distributed uniformly throughout the polymer chains, which results in a more consistent effect on free volume. The salt-free polymers range in T_g from 0.9 to −33.2 °C. In all instances, the T_g values for the salt-free polymers **7**−**9** were higher than their salt-containing counterparts.

Type C copolymers with dissolved salt (**7**−**9**) had T_g values between −27.9 and −32.5 °C. The salt-free polymers had values that ranged from −14.8 to −25.9 °C. Both ranges corresponded to a decreasing T_g with increasing alkyl ether incorporation.

Ionic Conductivities of Polymer−Salt Systems. The ratios of alkyl ether to trifluoroethoxy groups were varied in the different systems in an attempt to maximize both ionic conductivity and hydrophobicity of the solid polymers. Room-temperature conductivities are shown in Figure 5, and the results are compiled in Table 2.

The polymer blends (**14**−**16**) had very low conductivities compared to the Type B or Type C architectures. This is almost certainly a consequence of significant phase separation as indicated by the multiple T_g transitions. It was originally speculated that these polymers might give high conductivities if phase separation could be avoided because of the proximity between alkyl ether pendent groups on the same homopolymer chain and the possibility of channels of conductive groups within a hydrophobic matrix. This is the situation with proton conductors such as Nafion.[16] However, in this system, the hydrophobic domains appear to surround and insulate most of the conductive domains. Phase separation might possibly be overcome by crosslinking the polymers before phase separation can occur.

For the other systems, the ionic conductivity increased with the increasing incorporation of methoxyethoxyethoxy side groups. One of the more interesting trends was the dramatic increase in conductivity for the Type B polymers. Polymer **13** with only 40% alkyl ether incorporation had a conductivity similar to that of polymer **10** with 100% alkyl ether units. This result was consistent for experiments with several different samples of this polymer (± 29 nS/cm). The Nyquist plot for polymer **13** is shown in Figure 6.

Type C polymers showed a more linear relationship between conductivity and methoxyethoxyethoxy incorporation, ranging from 2106 nS/cm for polymer **7** to 6973 nS/cm for polymer **9**. The conductivities of polymers **7** and **8** were higher than those of their type B counterparts for the same side group ratios.

An interesting note is that polymer **6** (0% alkyl ether incorporation) has a conductivity of 1461 nS/cm. This is higher than for polymer **11** (Type B architecture, 10% alkyl ether groups), which may be a consequence of all the coordinative oxygen sites being saturated by coordination to cations at low alkyl ether loadings. Thus, the number of vacant oxygen sites may be too few to allow appreciable cation transfer.

Water Contact Angles. Water contact angles (WCAs) were measured to estimate the hydrophobicity of the polymer membranes. The WCAs of salt-free and salt-containing polymers were different because of the hydrophilicity of the salt. WCA values for the polymer systems are given in Table 2. In general, increasing loadings of alkyl ether groups led to lower contact angles, regardless of the inclusion of salt. The WCA results for salt-containing polymers are plotted in Figure 7.

The salt-containing polymer blends (Type A, **14-16**) had semi-hydrophobic surfaces initially, but the WCA decreased dramatically during several subsequent minutes. This is attributed to the hydrophilic side group migrating to the surface. The contact angles of salt-containing polymers **14**−**16** varied with time in contact with the water droplet, and the initial and final contact angles are reported for these polymers. Significant segmental motion occurs in these polymers (the polymers are well above their T_g values). This change in WCA was observed repeatedly and at roughly the same rate for each polymer blend. The same effect was observed for the salt-free WCAs, although the initial WCAs were higher than their salt-containing counterparts.

Type B polymers (**11**−**13**) had semi-hydrophobic surfaces with values similar to each other, ranging from 85.5 to 77.7°. Although polymer **11** had a WCA value that was lower than that of its type C counterparts, polymers **12** and **13** had WCA values that were significantly higher. It is noteworthy that a 40% alkyl ether loading in a type B polymer (polymer **13**, WCA = 77.7°) generated a significantly more hydrophobic surface than the corresponding arrangement in the Type A counterpart (polymer **9**, WCA = 36.2°) and still maintained significant conductivity. The same trend was observed for the salt-free polymers. The WCAs ranged from 86.0 to 82.1°.

Type C polymers (**7**−**9**) with salt had WCAs values that decreased dramatically from 91.3 to 36.2° as the alkyl ether loading increased. Polymer **7** with salt had the highest contact angle of all the (Type C) mixed-substituent polymers, being quite close to that of polymer **6** (100% trifluoroethoxy side groups). The WCA values for these Type C systems did not

(16) Mauritz, K. A.; Gray, C. L. *Macromolecules* **1983**, *17*, 1279.

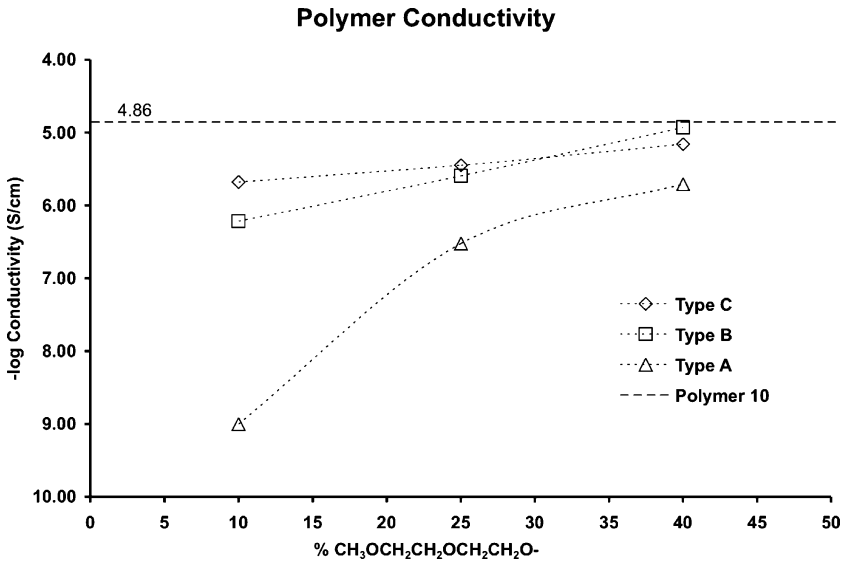

Figure 5. Polymer conductivity of salt-containing polymers.

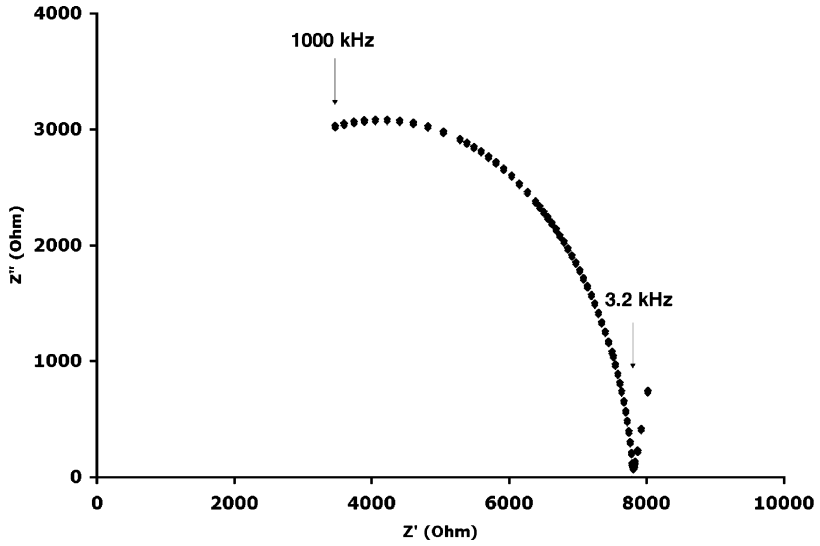

Figure 6. Nyquist plot of polymer **13**.

change after the water droplet was placed on the polymer film. This suggests that no significant concentrations of methoxyethoxyethoxy groups were present at the surface from the beginning and no migration to the surface took place. The same trend was observed for the salt-free polymers. The WCAs ranged from 95.6 to 50.9°.

The most conductive polymer−salt system (polymer **10**) was completely soluble in water (contact angle 0°).

Conclusions

Clearly, the different polymer systems give rise to significantly different properties. First, the properties of salt-containing, blended, single-substituent (Type A) polymers are a consequence of widespread phase separation. This is detrimental to both conductivity and hydrophobicity. The phase separation generates a significant barrier to ionic conductivity because each ionic conductive domain is separated by a relatively large distance from its neighbors, which makes the barrier to ion transport too high for adequate conductivity. This phase separation also has a significant effect on the WCA, with a drastic change in WCA immediately after a water droplet is brought into contact with the polymer surface. This change suggests either a rapid migration of hydrophilic domains to the surface or the permeation of water into the hydrophilic phases.

The differences between the behavior of the Types B and C architectures are significant and can be understood in terms of the pattern of distribution of the two types of functional units along the polymer chains. Much of the pendent unit and backbone reorganization that can occur with type C polymers is avoided with the type B architecture. In type B polymers, because every pendent group bears the same specific ratio of functional side units, any reorientation should only occur within a limited, perhaps nanometer scale region. This is indicated by much of the characterization data obtained for the type B polymers. Multiple hydrophobic units surround each hydrophilic unit because of the fixed side group ratios on each phosphazene ring. This creates an initial barrier to ion transport, although once the percolation threshold is surpassed, conductivity should occur readily. It is important to note that at a ratio of 40% methoxyethoxyethoxy units to 60% trifluoroethoxy groups (polymer **13**),

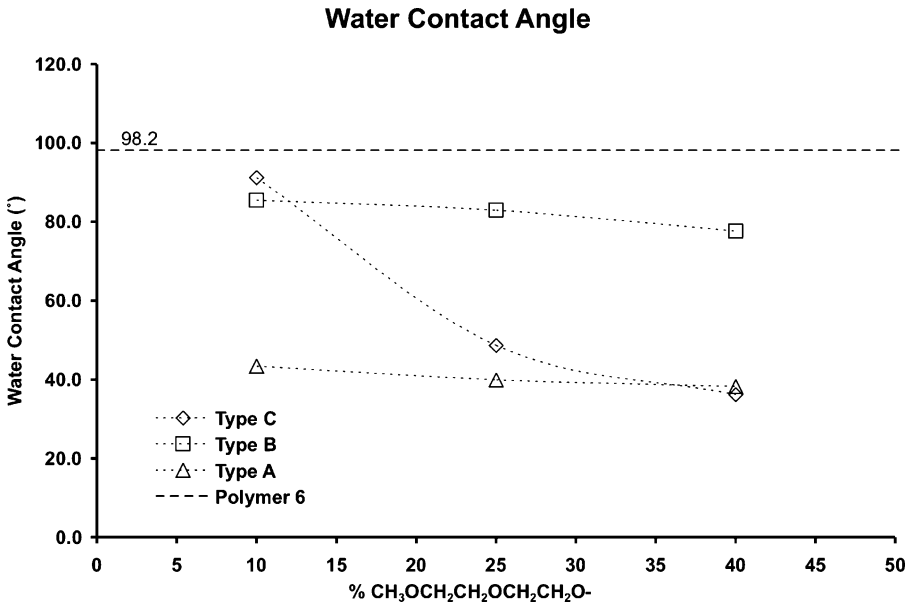

Figure 7. Water contact angle of salt-containing polymers.

the conductivity is quite close to that of the 100% methoxyethoxyethoxy system (polymer **10**). In addition, the surface characteristics of the type B polymers are more consistent throughout the range of compositions than with the type A architecture. Although a significant portion of alkyl ether units is present at the surface, a majority of hydrophobic groups are always present to prevent significant water permeation. Note that although polymer **10** with salt has a high ionic conductivity, it is soluble in water, whereas polymer **13** retains a semi-hydrophobic surface character.

The assembly of copolymers with type C architecture was affected by monomer/polymer/catalyst interactions. The dramatic decrease in molecular weight between polymers **7**−**9** illustrates the effect. If extended to include polymers **6** and **10** (homogeneous polymers), a clear trend is evident that the alkyl ether units decrease the activity of the catalyst. It is unclear whether this is merely a steric effect associated with the long alkyl ether units or a parasitic coordination with the ROMP catalyst. With respect to the influence of composition on physical properties, the T_g values of Type C polymers decreased from polymer **7** to **9**, but the methoxyethoxyethoxy pendent groups appeared to have only a limited influence on the T_g, by lowering it to a value around −30 °C when 10−40% of these groups were present. The same localized effect is seen in the conductivity, where only a modest increase occurs in ionic conductivity between polymer **7** (10% alkyl ether) and **8** (25% alkyl ether). It is possible that this is a result of reorientation of pendent groups to separate the hydrophobic and hydrophilic regions at the molecular level. This reorientation may yield microchannels of hydrophilic groups capable of producing higher-than-expected conductivity. However, at higher trifluoroethoxy incorporation, the microphase separation limits the conductivity. Even if multiple conductive microchannels aggregate, hydrophobic fluorine-rich regions will still surround them, preventing adequate conductivity. This local congregation of alkyl ether pendent groups may also lower the hydrophobicity of the surface.

These materials serve as a first step toward the production of a highly ionic conductive polymer that is resistant to water ingress. Specific polymers combine two opposing properties, ionic conduction and water resistance, into a single material that should prevent catastrophic failure of a lithium battery in a humid environment. Further improvements in performance may be necessary to produce a material capable of significant ionic conduction while being completely immersed in water for long periods of time. These improvements will probably be made through lamination or other engineering of the final device.

Experimental Section

Materials. All chemicals and reagents were obtained from Aldrich and used as received unless described otherwise. Hexachlorocyclotriphosphazene (Ethyl Corp./Nippon Fine Chemical Co.) was recrystallized from heptane and sublimed at 40 °C (0.05 mmHg). (±)-Meso-5-norbornene-2-methanol was synthesized as described previously.[17] Solvents were dried using an activated alumina column to remove protic contaminants. A supported copper catalyst (Q-5) was employed to remove dissolved oxygen from hydrocarbons.[18] *N*,*N*-Dimethylformamide (DMF) was purchased in a septa sealed bottle from EM Science. Lithium tetrafluoroborate ($LiBF_4$) was purchased from Aldrich, stored in a glovebox, and used unpurified.

Equipment. High-field ^1H (360.4 MHz), ^{13}C (90.56 MHz), and ^{31}P (145.79 MHz) NMR spectra were obtained using a Bruker AMX-360 spectrometer. ^{31}P NMR spectra were referenced to external 85% H_3PO_4 with positive shifts recorded downfield from the reference. ^1H and ^{13}C NMR spectra were referenced to the deuterated solvent resonances. Gel permeation chromatograms were obtained using a Hewlett-Packard HP 1090 gel permeation chromatograph equipped with two Phenomenex Phenogel linear 10 columns and a Hewlett-Packard 1047A refractive index detector. Data collection and calculations were accomplished with use of a Hewlett-Packard Chemstation equipped with Hewlett-Packard and

(17) Blanco, J. M.; Fernández, F.; García-Mera, X.; Rodríguez-Borges, J. *Tetrahedron* **2002**, *58*, 8843.
(18) Pangborn, A. B.; Giardello, M. A.; Grubbs, R. H.; Rosen, R. K.; Timmers, F. J. *Organometallics* **1996**, *15*, 1518.

Polymer Laboratories software. The samples were eluted at 1.0 mL/min with a 10 mM solution of tetra-*n*-butylammonium nitrate in THF. The elution times were referenced to polystyrene standards. Differential scanning calorimetry was performed using a TA Instruments DSCQ10 differential scanning calorimeter. Polymer samples were heated from −120 to 100 °C under an atmosphere of dry nitrogen. A typical heating rate of 10 °C/min, with sample sizes of 10-20 mg. Conductivity measurements were made using a Hewlett-Packard 4192A LF impedance analyzer at a potential of 0.1V with an alternating frequency range of 800 Hz to 1 MHz. The samples were placed between platinum electrodes separated by a Teflon spacer. The platinum electrode polymer−salt complexed cell was compressed between aluminum blocks held in a Teflon fixture. Electrical leads were attached between the impedance analyzer and the aluminum with a shorting three-way switch used to zero the instrument. Impedance of two identical films were measured and averaged for each polymer. Static water-contact angle measurements were obtained using a Rame-Hart model 100-00 contact-angle goniometer. Five static water-contact angles were obtained at room temperature with and without salt for each solid polymer electrolyte.

Synthesis. *Synthesis of 5-Norbornene-2-methanol.* Dicyclopentadiene was cracked at 180 °C and the evolved cyclopentadiene was collected and cooled to −78 °C. Acrolein (672.7 g, 12 mol) was added to a 1 L three-necked flask and cooled in an ice bath. Cyclopentadiene (793.2 g, 12 mol) was added dropwise by a dry-ice-cooled addition funnel. The reaction mixture was allowed to warm to room temperature for 2 h and then warmed to 45 °C and allowed to react for 8 h. Excess reactants were removed by distillation. Thin layer chromatography indicated a complete reaction. A portion of the resulting 5-norbornene-2-aldehyde (500 g, 4.1 mol) was diluted with 2 L of methanol and cannulated into a cold suspension of sodium borohydride (79.0 g, 2.0 mol) and 2 M sodium hydroxide. The reaction mixture was warmed to room temperature and stirred for 1 h. The solvent was removed by rotary evaporation, and the remaining products were dissolved in diethyl ether (600 mL), washed with aqueous sodium carbonate (2 × 750 mL) and water (750 mL), dried over magnesium sulfate, filtered, and isolated by rotary evaporation. The product was isolated and dried overnight under a vacuum to give pure 5-norbornene-2-methanol (348.7 g, 68.6%). ^{1}H NMR ($CDCl_3$): δ 6.15 (q, J = 2.9 Hz, 5-H, endo, 0.7 H), 6.11 (q, J = 2.9 Hz, 5-H, exo, 0.3 H), 6.08 (q, J = 2.9 Hz, 6-H, exo, 0.3 H), 5.96 (q, J = 2.9 Hz, 6-H, endo, 0.7 H), 3.71 (dd, J = 6.4, 10.5 Hz, −CH_2O−, exo, 0.3 H), 3.54 (dd, J = 8.8, 10.5 Hz, −CH_2O−, exo, 0.3 H), 3.40 (dd, J = 6.5, 10.4 Hz, −CH_2O−, endo, 0.7 H), 3.26 (dd, J = 9.0, 10.4 Hz, −CH_2O−, endo, 0.7 H), 2.93 (s, 1-H, endo, 0.7 H), 2.82 (s, 4-H, endo, 0.7 H), 2.75 (s, 4-H, exo, 0.3 H), 2.30 (m, 2-H, endo, 0.7 H), 1.82 (ddd, J = 3.7, 9.1, 11.6 Hz, 3-H, endo, 0.7 H), 1.62 (m, 2-H, exo, 0.3 H), 1.61 (m, 2-H, exo, 0.3 H), 1.45 (dt, J = 2.1, 6.2 Hz, 7-H, endo, 0.3 H), 1.32 (q, 1-H, exo, 0.3 H), 1.27 (resolved with HMQC) (t, 7-H, exo, 0.3 H), 1.25 (t, 3-H, exo, 0.3 H), 1.11 (dt, J = 3.9, 11.6 Hz, 3-H, exo, 0.3 H), 0.53 (ddd, J = 2.6, 4.4, 11.6 Hz, 3-H, endo, 0.7 H). ^{13}C NMR ($CDCl_3$): δ 137.27 (5-C, endo), 136.67 (5-C, exo), 136.62 (6-C, exo), 132.27 (6-C, endo), 67.04 (−*C*H_2O−, exo), 66.06 (−*C*H_2O−, endo), 49.48 (7-C, exo + endo), 44.91 (1-C, exo), 43.59 (4-C, endo), 43.30 (4-C, exo), 42.21 (1-C, endo), 41.68 (2-C, exo), 41.54 (2-C, endo), 29.58 (3-C, exo), 28.88 (3-C, endo).

*Synthesis of (NBO)(PN)$_3$(Cl)$_5$ (**2**).* A 2 L three-necked flask was charged with potassium tert-butoxide (69.166 g, 0.6041 mol) that was dissolved in ∼1.5 L THF. (±)-Meso-5-norbornene-2-methanol (75.01 g, 0.6041 mol) was then added to the flask and allowed to react for ∼12 h to ensure the completion of the reaction. Hexachlorocyclotriphosphazene (300 g, 0.8629 mol) was added to a 5 L three-neck flask and dried under a vacuum for an hour. The cyclotriphosphazene was then dissolved in ∼3 L of THF. Both mixtures were cooled to −78 °C in an isopropanol/ dry ice bath. The norbornene salt solution was then added by cannula to the cyclotriphosphazene solution in a constant dropwise stream. Once the addition was complete, the mixture was allowed to warm to room temperature and was stirred for ∼12 h. The reaction mixture was monitored by ^{31}P NMR spectroscopy to ensure complete substitution. The products were isolated by rotary evaporation, dissolved in ether (∼750 mL), and washed several times with water (3 × 700 mL). The organic layer was collected, dried with $MgSO_4$, filtered, and isolated by rotary evaporation. The resulting tan gel was dried under a vacuum to remove excess solvent and then placed in a vacuum sublimator. Excess hexachlorocyclotriphosphazene was removed via sublimation at 40 °C at 0.01 mmHg for 2 days. The resultant dark liquid was collected resulting in 257.24 g (97.8%) of product. ^{31}P NMR spectroscopy indicated the existence of a pure product with less than 1% hexachlorocyclotriphosphazene. ^{31}P NMR ($CDCl_3$): δ 22.75 (d, J = 61.6 Hz, -*P*($Cl)_2$, 2P), 14.90 (t, J = 62.0 Hz, −P(Cl)(*exo*-ONB), 0.3 P), 14.61 (t, J = 62.0 Hz, -P(Cl)(*endo*-ONB), 0.7 P). ^{1}H NMR ($CDCl_3$): δ 6.20 (q, J = 2.9 Hz, 5-H, endo, 0.7 H), 6.11 (m, 5-H, exo, 0.3 H), 6.11 (m, 6-H, exo, 0.3 H), 6.01 (q, J = 2.8 Hz, 6-H, endo, 0.7 H), 4.26 (ddd, J = 6.4, 8.4, 8.9 Hz, −CH_2O−, exo, 0.3 H), 4.08 (dd, J = 9.6, 19.2 Hz, −CH_2O−, exo, 0.3 H), 3.97 (m, −CH_2O−, endo, 0.7 H), 3.77 (dd, J = 9.8, 19.5 Hz, −CH_2O−, endo, 0.7 H), 2.99 (s, 1-H, endo, 0.7 H), 2.86 (s, 4-H, endo, 0.7 H), 2.82 (s, 4-H, exo, 0.3 H), 2.53 (m, 2-H, endo, 0.7 H), 1.89 (ddd, J = 3.7, 8.8, 11.9 Hz, 3-H, endo, 0.7 H), 1.89 (m, 2-H, exo, 0.3 H), 1.50 (dm, J = 8.4 Hz, 7-H, endo, 0.3 H), 1.40 (m, 1-H, exo, 0.3 H), 1.31 (t, 7-H, exo, 0.3 H), 1.30 (t, 3-H, exo, 0.3 H), 1.20 (m, 3-H, exo, 0.3 H), 0.53 (ddd, J = 2.6, 4.4, 11.6 Hz, 3-H, endo, 0.7 H). ^{13}C NMR ($CDCl_3$): δ 138.03 (5-C, endo), 137.13 (5-C, exo), 136.00 (6-C, exo), 131.92 (6-C, endo), 73.36 (−*C*H_2O−, exo), 72.82 (−*C*H_2O−, endo), 49.32 (7-C, exo + endo), 44.82 (1-C, exo), 43.59 (4-C, endo), 43.26 (4-C, exo), 42.23 (1-C, endo), 41.58 (2-C, exo), 38.76 (2-C, endo), 29.218 (3-C, exo), 28.56 (3-C, endo).

Monomer Synthesis. *General Synthesis of Homogeneous Monomers (NBO)(PN)$_3$(OR)$_5$.* A 500 mL flask was charged with potassium tert-butoxide (5.5 equiv), which was dissolved in ∼400 mL of THF. The appropriate alcohol (5.5 equiv) was added to the suspension and allowed to react for ∼12 h to ensure a complete reaction. Compound **2** (1 eq) was added to a dry 1 L three-neck flask and dissolved in ∼500 mL THF. The salt solution was added to compound **2** solution by cannula in a constant stream. It was necessary in many instances to place the three-necked flask in a cold-water bath because of the evolution of heat. The reaction was allowed to proceed for ∼12 h, and ^{31}P NMR spectra were taken to ensure the completion of the reaction. The products were isolated by rotary evaporation and redissolved in ether. The product was then washed several times with water. Several of the monomers, when washed, produced an emulsion with little or no phase separation. Phase separation could be induced by the addition or use of a 1% $HCl_{(aq)}$ solution for liquid−liquid extraction. The organic layer was then collected, dried with $MgSO_4$, filtered, and isolated by rotary evaporation to give a viscous liquid. Typical yields were >95%.

*[(5-Norbornene-2-methoxy)penta(2,2,2-trifluoroethoxy)]cyclotriphosphazene (**3a**).* ^{31}P NMR ($CDCl_3$): δ 18.28 (m, 3P). ^{1}H NMR ($CDCl_3$): δ 6.17 (q, J = 2.9 Hz, 5-H, endo, 0.7 H), 6.11 (q, 5-H, exo, 0.3 H), 6.08 (q, 6-H, exo, 0.3 H), 5.95 (q, J = 2.9 Hz, 6-H, endo, 0.7 H), 4.26 (m, −CH_2CF_3, exo + endo, 10 H) 4.04 (dt, J = 6.5, 9.8 Hz, −CH_2O−, exo, 0.3 H), 3.88 (dt, J = 7.2, 9.7 Hz,

−CH_2O−, exo, 0.3 H), 3.73 (dt, J = 6.5, 9.6 Hz, −CH_2O−, endo, 0.7 H), 3.58 (dt, J = 7.5, 9.6 Hz, −CH_2O−, endo, 0.7 H), 2.92 (s,1-H, endo, 0.7 H), 2.84 (s, 4-H, endo, 0.7 H), 2.75 (s, 4-H, exo, 0.3 H), 2.45 (m, 2-H, endo, 0.7 H), 1.82 (ddd, J = 3.8, 9.1, 11.6 Hz, 3-H, endo, 0.7 H), 1.78 (m, 2-H, exo, 0.3 H), 1.49 (dt, J = 2.1, 6.2 Hz, 7-H, endo, 0.3 H), 1.40−1.20 (1-H exo, 7-H exo, 3-H exo, unresolved) 1.11 (dt, J = 3.9, 11.6 Hz, 3-H, exo, 0.3 H), 0.53 (ddd, J = 2.6, 4.4, 11.6 Hz, 3-H, endo, 0.7 H). ^{13}C NMR ($CDCl_3$): δ 138.1 (5-C, endo), 136.1 (5-C, exo), 136.1 (6-C, exo), 132.0 (6-C, endo), 121.3 (q, J = 278 Hz, −OCH$_2$CF_3), 71.7 (−CH_2O−, exo), 71.1 (−CH_2O−, endo), 63.2 (qd, J = 16.2, 39.6 Hz, −CH_2-CF_3), 49.58 (7-C, exo + endo), 44.95 (1-C, exo), 43.88 (4-C, endo), 43.54 (4-C, exo), 42.47 (1-C, endo), 41.80 (2-C, exo), 39.49 (d, J = 7.3 Hz, 2-C, + endo), 39.29 (d, J = 7.8 Hz, 2-C, endo), 29.40 (3-C, exo), 28.78 (3-C, endo). APCI+ m/z: 753.9 (MH+).

*[(5-Norbornene-2-methoxy)penta(2-(2-methoxyethoxy)ethoxy)] cyclotriphosphazene (**3b**).* ^{31}P NMR ($CDCl_3$): δ 18.08 (m, 3P). ^{1}H NMR ($CDCl_3$): δ 6.05 (q, 5-H, endo, 0.7 H), 6.00 (m, 5-H ,exo, 0.3 H), 5.99 (q, 6-H, exo, 0.3 H), 5.91 (q, 6-H, endo, 0.7 H), 3.98 (bm, −OCH_2CH$_2$−, 10H), 3.62 (bm, −OCH$_2$CH_2−, 10H), 3.56 (bm, −OCH_2CH$_2$OCH$_3$, 10H), 3.44 (bm,−OCH$_2$CH_2OCH$_3$, 10H), 3.30 (s, −OCH_3, 15 H), 4.0−3.2 (unresolved, −CH_2O− exo + endo, 2H), 2.87 (s,1-H, endo, 0.7 H), 2.72 (s, 4-H, endo, 0.7 H), 2.46 (s, 4-H, exo, 0.3 H), 2.36 (m, 2-H, endo, 0.7 H), 1.72 (m, 3-H, endo, 0.7 H), 1.70−1.08 (2-H exo, 7-H endo, 1-H exo, 7-H exo, 3-H exo, unresolved), 0.43 (ddd, 3-H, endo, 0.7 H). ^{13}C NMR ($CDCl_3$): δ 136.9 (5-C, endo), 136.5 (5-C, exo), 136.0 (6-C, exo), 132.1 (6-C, endo), 71.56 (−OCH$_2$CH_2O−), 70.17 (−OCH_2CH$_2$-OCH$_3$), 69.98 (−CH_2O−), 69.65 (−OCH$_2$CH_2OCH$_3$), 64.64 (−OCH_2CH$_2$O−), 58.64 (−OCH_3), 48.90 (7-C, exo + endo), 44.52 (1-C, exo), 43.33 (4-C, endo), 43.02 (4-C, exo), 41.86 (1-C, endo), 41.21 (2-C, exo), 38.82 (m, 2-C, endo), 28.92 (3-C, exo), 28.32 (3-C, endo). APCI+ *m*/*z*: 854.2 (MH+).

General Synthesis of Mixed-Substituent Monomers (3c, 3d, or 3e). A 500 mL flask was charged with potassium tert-butoxide (5.0 equiv.), which was dissolved in THF. 2-(2-Methoxyethoxy)-ethanol (y equiv.; see Figure 3) was added to the solution all at once and allowed to react for several hours, after which 2,2,2-trifluoroethanol (z eq) was added. This reaction was allowed to proceed for 12 h to ensure completion of the reaction. Compound **2** was added to a 1 L three-neck flask and dissolved in THF. The salt solution was then added to the solution of compound **2** via cannula. The reaction was exothermic and was allowed to proceed for ∼12 h to ensure complete conversion. The reaction products were isolated by rotary evaporation and then dissolved in ether (250 mL). The product was washed several times with water. Several of the monomers when washed gave an emulsion with little or no phase separation. Phase separation could be induced by the addition or use of a 1% $HCl_{(aq)}$ solution for liquid−liquid extraction. The organic layer was then collected, dried with $MgSO_4$, filtered, and isolated by rotary evaporation to give a viscous liquid. The purity of the liquid was confirmed by ^{31}P NMR, ^{1}H NMR, and AP-MS. Mass spec showed a statistical distribution of monomers, NMR showed the desired ratio was achieved (± 4%). Yields were typically greater than 90%.

*[(5-Norbornene-2-methoxy)$_1$ (2,2,2-trifluoroethoxy)$_{4.5}$ (2-(2-methoxyethoxy)ethoxy)$_{0.5}$]cyclotriphosphazene (**3c**).* Target composition: 10.0% MEE/90.0% TFE. Actual composition: 10.2% MEE/89.8% TFE. ^{31}P NMR ($CDCl_3$): δ 17.52 (m, 3P). ^{1}H NMR ($CDCl_3$): δ 6.17 (q, 5-H, endo, 0.7 H), 6.10 (q, 5-H, exo, 0.3 H), 6.10 (q, 6-H, exo, 0.3 H), 5.94 (q, 6-H, endo, 0.7 H), 4.26 (m, −CH_2CF_3, 8.8 H) 4.2−3.4 (−OCH_2CH$_2$−, −OCH$_2$CH_2−, −CH_2-CH$_2$OCH$_3$, −OCH$_2$CH_2OCH$_3$, NBCH$_2$O− exo + endo), 3.36 (s, −OCH$_3$, 1.5 H), 2.92 (s,1-H, endo, 0.7 H), 2.84 (s, 4-H, endo, 0.7 H), 2.75 (s, 4-H, exo, 0.3 H), 2.44 (m, 2-H, endo, 0.7 H), 1.82 (m, 3-H, endo, 0.7 H), 1.78 (m, 2-H, exo, 0.3 H), 1.49 (m, 7-H endo, 0.3 H), 1.40−1.20 (1-H exo, 7-H exo, 3-H exo, unresolved) 1.11 (dt, 3-H, exo, 0.3 H), 0.53 (m, 3-H, endo, 0.7 H). ^{13}C NMR ($CDCl_3$): δ 137.75 (m, 5-C, endo), 137.08 (5-C, exo), 136.1 (6-C, exo), 131.89 (m, 6-C, endo), 122.53 (bq, J = 278 Hz, −OCH$_2$CF_3), 71.76 (−OCH$_2$CH_2O−), 70.81 (−CH_2O−, endo), 70.50 (−OCH_2-CH$_2$OCH$_3$), 69.71 (m, −OCH$_2$CH_2OCH$_3$), 65.91 (m, −CH_2CF_3), 62.62 (bm, −OCH_2CH$_2$O−), 58.80 (−OCH_3), 49.21 (7-C, exo + endo), 44.63 (1-C, exo), 43.55 (4-C, endo), 43.23 (4-C, exo), 42.17 (1-C, endo), 41.49 (2-C, exo), 39.00 (m, 2-C, endo), 29.06 (3-C, exo), 28.46 (3-C, endo).

*[(5-Norbornene-2-methoxy)$_1$ (2,2,2-trifluoroethoxy)$_{3.75}$ (2-(2-methoxyethoxy)ethoxy)$_{1.25}$]cyclotriphosphazene (**3d**).* Target composition: 25% MEE/75% TFE. Actual composition: 27.0% MEE/73.0% TFE. ^{31}P NMR ($CDCl_3$): δ 17.32 (m, 3P), ^{1}H NMR ($CDCl_3$): δ 6.15 (q, 5-H, endo, 0.7 H), 6.10 (q, 5-H, exo, 0.3 H), 6.10 (q, 6-H, exo, 0.3 H), 5.95 (q, 6-H, endo, 0.7 H), 4.26 (bm, −CH_2CF_3, 7.7 H) 4.2−3.4 (−OCH_2CH$_2$−, −OCH$_2$CH_2−, −CH_2-CH$_2$OCH$_3$, −OCH$_2$CH_2OCH$_3$, NBCH$_2$O− exo + endo), 3.36 (s, −OCH$_3$, 4.5 H), 2.92 (s,1-H, endo, 0.7 H), 2.82 (s, 4-H, endo, 0.7 H), 2.75 (s, 4-H, exo, 0.3 H), 2.44 (m, 2-H, endo, 0.7 H), 1.82 (m, 3-H, endo, 0.7 H), 1.78 (m, 2-H, exo, 0.3 H), 1.49 (m, endo, 0.3 H), 1.40−1.20 (1-H exo, 7-H exo, 3-H exo, unresolved), 1.11 (dt, 3-H, exo, 0.3 H), 0.50 (m, 3-H, endo, 0.7 H). ^{13}C NMR ($CDCl_3$): δ 137.65 (m, 5-C, endo), 136.94 (5-C, exo), 135.95 (6-C, exo), 131.80 (m, 6-C, endo), 122.57 (q, J = 278 Hz, −OCH$_2$CF_3), 71.73 (−OCH$_2$CH_2O−), 70.75 (−CH_2O−, endo), 70.48 (−OCH_2CH$_2$-OCH$_3$), 69.67 (m, −OCH$_2$CH_2OCH$_3$), 65.87 (m, −CH_2CF_3), 62.58 (bm, −OCH_2CH$_2$O−), 58.76 (−OCH_3), 49.21 (7-C, exo + endo), 44.61 (1-C, exo), 43.52 (4-C, endo), 43.17 (4-C, exo), 42.11 (1-C, endo), 41.45 (2-C, exo), 38.96 (m, 2-C, endo), 29.04 (3-C, exo), 28.44 (3-C, endo).

*[(5-Norbornene-2-methoxy)$_1$ (2,2,2-trifluoroethoxy)$_3$ (2-(2-methoxyethoxy)ethoxy)$_2$]cyclotriphosphazene (**3e**).* Target composition: 40% MEE/60% TFE. Actual composition: 43.2% MEE/56.8% TFE. ^{31}P NMR ($CDCl_3$): δ 17.55 (m, 3P), ^{1}H NMR ($CDCl_3$): δ 6.13 (q, endo, 0.7 H), 6.06 (q, 5-H, exo, 0.3 H), 6.06 (q, 6-H, exo, 0.3 H), 5.94 (q, 6-H, endo, 0.7 H), 4.24 (bm, −CH_2-CF_3, 5.7 H), 4.2−3.4 (−OCH_2CH$_2$−, −OCH$_2$CH_2−, −CH_2CH$_2$-OCH$_3$, −OCH$_2$CH_2OCH$_3$, NBCH$_2$O− exo + endo), 3.35 (s, −OCH$_3$, 6.5 H), 2.90 (s, 1-H, endo, 0.7 H), 2.80 (s, 4-H, endo, 0.7 H), 2.75 (s, 4-H, exo, 0.3 H), 2.42 (m, 2-H, endo, 0.7 H), 1.82 (m, 3-H, endo, 0.7 H), 1.78 (m, 2-H, exo, 0.3 H), 1.45 (m, 7-H endo, 0.3 H), 1.40−1.20 (1-H exo, 7-H exo, 3-H exo, unresolved) 1.11 (dt, 3-H, exo, 0.3 H), 0.50 (m, 3-H, endo, 0.7 H). ^{13}C NMR ($CDCl_3$): δ 137.49 (m, 5-C, endo), 136.77 (5-C, exo), 135.93 (6-C, exo), 131.80 (6-C, endo), 122.6 (q, J = 278 Hz, −OCH$_2$CF_3), 71.86 (−OCH$_2$CH_2O−), 70.31 (−OCH_2CH$_2$OCH$_3$), 70.06 (−CH_2O−, endo), 69.48 (m, −OCH$_2$CH_2OCH$_3$), 65.50 (m, −CH_2-CF_3), 62.39 (bm, −OCH_2CH$_2$O−), 58.56 (−OCH_3), 49.07 (7-C, exo + endo), 44.51 (1-C, exo), 43.38 (4-C, endo), 43.08 (4-C, exo), 41.99 (1-C, endo), 41.33 (2-C, exo), 38.83 (m, 2-C, endo), 28.94 (3-C, exo), 28.31 (3-C, endo).

Polymerization. *General Ring-Opening Metathesis Polymerization of Single- and Mixed-Substituent Monomers.* At room temperature, the appropriate monomer or mixture of monomers was dissolved in THF (1 mL/ 0.2 g of monomer) within a 100 mL three-neck flask. First generation Grubbs' catalyst (250/1 = [monomer]/[1]) was dissolved in 0.9 mL of CH_2Cl_2 and added to the reaction solution as quickly as possible. Addition of the initiator induced a color darkening in each reaction mixture. Each polymerization was allowed to proceed until a change of viscosity was detected, after which the reaction was terminated with a BHT/ ethylvinylether

solution (1.0 mL). This was allowed to react for 30 min. The polymerization product was transferred to dialysis tubing (MWCO = 12 000−14 000) and dialyzed against THF for several days. Once dialysis was finished, the purified polymer was then concentrated by rotary evaporation to the point where precipitation occurred; the polymer solution was then precipitated into a non-solvent, typically hexanes. The polymer was then collected and dried under a vacuum at 60 °C for 24 h. Typical yields were higher than 80%.

Polymer Characterization. The polymers were characterized by ^{31}P, ^{1}H, and ^{13}C NMR spectroscopy. All shifts are reported from TMS, and the integration is per repeat unit. To detect many of the vinyl (backbone) carbon peaks, we significantly reduced the relaxation time of the carbon spectra ($d1 = 0.1-0.4$ s). All carbon spectra showed broadening of the backbone peaks and significant overlap of peaks due to partial solubility and regioisomers of the repeat units. Because of this, we do not report ^{13}C NMR characterization for all polymers.

*Polymer **6***. ^{31}P NMR (d_7-DMF): δ 17.77 (br). ^{1}H NMR (d_7-DMF): δ 5.42 (br, olefin, trans, 1H), 5.32 (br, olefin, cis, 1H), 4.67 (bm, $-CH_2CF_3$, 10 H), 4.02 ($NBCH_2O-$, exo + endo), 3.46 (br,1-H endo, 4-H endo), 3.11 (bm, 4-H, exo), 2.40 (m, 2-H, endo), 2.2−1.0 (bm, 3-H endo, 2-H exo, 7-H endo,1-H exo, 7-H exo, 3-H exo, unresolved), 0.50 (bm, 3-H, endo). ^{13}C NMR (d_7-DMF): δ 136.2 (5-C), 130.1 (6-C), 124.6 (q, $J = 277$ Hz, $-OCH_2CF_3$), 70.4 ($-CH_2O-$), 63.7 (td, $J = 36.6$, 36.7 Hz, $-CH_2CF_3$), 46.82, 45.38, 43.75, 42.3, 42.8, 41.3, 40.3, 40.0, 38.3, 37.6 (unassigned). 3-C could not be observed due to d_7-DMF peak at 31.5−29.9.

*Polymer **7***. ^{31}P NMR (d_7-DMF): δ 17.60 (br). ^{1}H NMR (d_8-THF): δ 5.39 (br, olefin, 2H), 4.44 (bm, $-CH_2CF_3$, 9.1 H), 4.2−3.8 ($NBCH_2O-$ exo + endo, $-OCH_2CH_2-$), 3.71 ($-OCH_2CH_2-$, 1H), 3.46 ($-CH_2CH_2OCH_3$, 1H), 3.38 ($-OCH_2CH_2OCH_3$, 1H), 3.29 (s, $-OCH_3$, 1.5 H), 2.69 (br,1-H, endo, 0.7 H), 2.47 (bs, 4-H, endo, 0.7 H), 2.75 (bs, 4-H, exo, 0.3 H), 2.43 (m, 2-H, endo, 0.7 H), 2.3−1.2 (bm, 3-H endo, 2-H exo, 7-H endo, 1-H exo, 7-H exo, 3-H exo, unresolved), 0.87 (bm, 3-H, endo, 0.7 H).

*Polymer **8***. ^{31}P NMR (d_7-DMF): δ 17.54 (br). ^{1}H NMR (d_7-DMF): δ 5.44 (br, olefin, 2H), 4.69 (bm, $-CH_2CF_3$, 7.5 H), 4.2−3.8 ($NBCH_2O-$), 3.67 ($-OCH_2CH_2-$, $-OCH_2CH_2-$, $-CH_2CH_2-OCH_3$, $-OCH_2CH_2OCH_3$), 3.29 (s, $-OCH_3$), 2.40 (2-H endo), 1.96 (3-H endo), 1.85 (2-H exo), 1.60 (1-H exo, 7-H endo), 1.26 (7-H exo, 3-H exo), 0.87 (3-H endo), (1-H endo, 4-H endo + exo could not be resolved due to d_7-DMF at 2.92−2.75).

*Polymer **9***. ^{31}P NMR (d_7-DMF): δ 17.82 (br). ^{1}H NMR (d_7-DMF): δ 5.47 (br, olefin, 2H), 4.69 (bm, $-CH_2CF_3$, 7.5 H), 4.2−3.8 ($NBCH_2O-$), 3.56 ($-OCH_2CH_2-$, $-OCH_2CH_2-$, $-CH_2CH_2-OCH_3$, $-OCH_2CH_2OCH_3$), 3.29 (s, $-OCH_3$), 2.42 (2-H endo), 1.96 (3-H endo), 1.85 (2-H exo), 1.60 (1-H exo, 7-H endo), 1.27 (7-H exo, 3-H exo), 0.87 (3-H endo), (1-H endo, 4-H endo + exo could not be resolved due to d_7-DMF at 2.92−2.75).

*Polymer **10***. ^{31}P NMR (d_7-DMF): δ 18.37 (br). ^{1}H NMR (d_7-DMF): δ 5.46 (br, olefin, 1H) 5.36 (br, olefin, 1H) 4.13 ($NBCH_2O-$ exo + endo, 2H), 4.05 (bm, $-OCH_2CH_2-$, 10H), 3.69 (bm, $-OCH_2CH_2-$, 10H), 3.61 (bm, $-OCH_2CH_2OCH_3$, 10H), 3.51 (bm, $-OCH_2OCH_3$, 10H), 3.31 (m, $-OCH_3$, 15 H), 4.0−2.6 ($-CH_2O-$ exo, $-CH_2O-$ endo, 1-H endo, 4-H endo, unresolved), 2.51 (m, 4-H, exo, 0.3 H), 2.41 (bm, 2-H, endo, 0.7 H), 2.02 (m, 3-H, endo, 0.7 H), 1.85−1.40 (2-H exo, 7-H endo, 1-H exo, 7-H exo, unresolved), 1.26 (br, 3-H exo, 0.3) 0.85 (t, 3-H, endo, 0.7 H).

*Polymer **11***. ^{31}P NMR (d_7-DMF): δ 17.77 (br). ^{1}H NMR (d_6-acetone): δ 5.44 (br, olefin, 2H), 4.56 (br, $-CH_2CF_3$, 9 H), 4.2−3.8 ($NBCH_2O-$ exo + endo, $-OCH_2CH_2-$), 3.71 ($-OCH_2CH_2-$, 1H), 3.62 ($-CH_2CH_2OCH_3$, 1H), 3.50 ($-OCH_2CH_2OCH_3$, 1H), 3.30 (s, $-OCH_3$, 1.5 H), 2.80 (br,1-H, endo, 0.7 H), 2.80 (bs, 4-H, endo, 0.7 H), 2.75 (bs, 4-H, exo, 0.3 H), 2.43 (m, 2-H, endo, 0.7 H), 2.3−1.2 (bm, 3-H, endo, 2-H, exo, 7-H endo,1-H exo, 7-H exo, 3-H exo, alkyl backbone), 0.87 (bm, 3-H, endo, 0.7 H).

*Polymer **12***. ^{31}P NMR (d_7-DMF): δ 17.67 (br). ^{1}H NMR (d_7-DMF): δ 5.44 (br, olefin, 2H), 4.61 (bm, $-CH_2CF_3$, 2H), 4.15 (br, $NBCH_2O-$, 1H), 4.01 (br, $NBCH_2O-$, 1H) 3.71 ($-OCH_2CH_2-$, 2H), 3.63 ($-OCH_2CH_2$, 2H) 3.61 ($-CH_2CH_2OCH_3$, 2H), 3.52 ($-OCH_2CH_2OCH_3$, 2H), 3.30 (s, $-OCH_3$, 3.75 H), 2.41 (bm, 2-H, endo, 1 H), 2.01 (br, 3-H, exo, 1H) 1.89 (br, 2-H, exo, 1H) 1.60 (br, 7-H, endo, 1H) 1.27 (br, 3-H exo, 7-H exo, 1-H exo), 0.87 (bm, 3-H, endo, 1 H).

*Polymer **13***. ^{31}P NMR (d_7-DMF): δ 17.84 (br). ^{1}H NMR (d_6-acetone): δ 5.5−5.2 (bd, olefin, 2H), 4.48 (bm, $-CH_2CF_3$, 5.6 H), 4.2−3.8 ($NBCH_2O-$ exo + endo, $-OCH_2CH_2-$), 3.70 ($-OCH_2CH_2-$, 1H), 3.62 ($-CH_2CH_2OCH_3$, 1H), 3.51 ($-OCH_2CH_2-OCH_3$, 1H), 3.30 (s, $-OCH_3$, 6.6 H), 2.77 (br, 1-H, endo, 0.7 H), 2.77 (bs, 4-H endo, 0.7 H), 2.70 (bs, 4-H exo, 0.3 H), 2.42(bm, 2-H, endo, 0.7 H), 2.3−1.2 (bm, 3-H endo, 2-H exo, 7-H endo,1-H exo, 7-H exo, 3-H exo, unresolved), 0.89 (bm, 3-H, endo, 0.7 H).

General Method for Polymer Blends with Salts 14−16. Polymers **6** and **10** were combined in 10 mL of DMF and thoroughly mixed until homogeneous. The DMF was allowed to evaporate slowly at room temperature and atmospheric pressure. The resultant film was then placed in a vacuum oven at 60 °C for 1 week. No NMR characterization was carried out for the mixed polymer series.

General Method for Film Casting. Each polymer and 7 wt % $LiBF_4$ were dissolved in 5 mL of DMF (2.5% w/w), allowed to equilibrate for 24 h, and then slowly deposited on a clean glass slide. Each glass slide was covered with a Petri dish to slow the evaporation of solvent. The samples were allowed to air-dry over several days. Once a stable film was formed, the samples were dried at 60−70 °C under a vacuum for 72 h to remove excess solvent.

CM062528U